A dimensionality reduction method to select the most representative daylight illuminance distributions

Michael G Kent*[a], **Stefano Schiavon**[b] and **John Alstan Jakubiec**[c]

[a] Berkeley Education Alliance for Research in Singapore, Singapore

[b] Center for the Built Environment, University of California, Berkeley, CA, USA

[c] John H. Daniels Faculty of Architecture, Landscape, and Design, University of Toronto, Canada

* Corresponding author: michaelkent@berkeley.edu

Abstract

One challenge when evaluating daylight distribution is dealing with the large amount of temporal and spatial data, visualisations and variability in illuminances that are assessed in buildings. Using a dimensionality reduction method based on principal component analysis, we identified the most representative annual daylight distributions. We modelled a rectangular room containing an analysis grid of 3200 illuminance sensor points and simulated 3285 different temporal daylight conditions using an annual occupancy schedule ranging from 08:00 to 17:00 with one-hour sampling intervals in two locations: Singapore and Oakland, California. Our approach explained 98 % of the illuminance variability with three daylight distributions in Singapore, and 92 % using six in Oakland, California. Our dimensionality reduction strategy was also generalised using a complex building geometry showing the utility of the method. We think this approach can be used to provide a more efficient and reliable method to analyse daylight performance in building practice.

Keywords: Daylight distribution; Illuminance; Principal components analysis; Simulation; Statistical analysis.

 https://doi.org/10.1080/19401493.2019.1711456
https://escholarship.org/uc/item/04x6v86j

1. Introduction

Illumination that is received on the horizontal work surface is designed so that it meets a certain minimum criterion, is uniformly distributed, and does not cause visual discomfort. These criteria are not always met, since daylight from side-lit openings can cause significant changes in the light levels received on the indoor surfaces (Constantatos, 1982). Daylight distribution is dependent on a number of variables, for example, how light interacts with the geometry of the building, building façade geometry and optical properties, and changes in the outdoor conditions (Lee *et al.*, 1999; Mardaljevic *et al.*, 2009). This creates a luminous environment that continuously undergoes dynamic changes.

Annual daylight metrics – commonly referred to as Climate-Based Daylight Metrics (CBDM) – have been developed to evaluate the performance of natural light inside buildings. These can be used to calculate a percentage time of the year in which daylight meets predefined targets based on meteorological weather data (e.g. Daylight Autonomy, Useful Daylight Illuminance, etc. (Nabil and Mardaljevic, 2006, 2005; Reinhart et al., 2006)). Since these summarise the performance of daylight into a single value, information regarding the distribution of daylight can be lost in these processes. Although it has been suggested that light distribution is an important design consideration (Boyce, 2014), there are limited daylight metrics that have been designed to evaluate a range of luminous effects that occur across the annual occupied hours of a building (Rockcastle and Andersen, 2014).

While the introduction of daylight in buildings can be used to indirectly offset electric lighting usage through the use of sensors and control systems (i.e., dimmers and illuminance sensors) (Kamaruzzaman *et al.*, 2015; Xue *et al.*, 2016), this is not only dependent on whether the daylight can meet – and does not exceed – the design illuminance value but also on its spatial distribution throughout the entire occupied space. In fact, Yun *et al.* (Yun *et al.*, 2012) suggests that energy use from artificial light can be reduced by 30 % when lighting controls are carefully designed in relation to indoor daylight distribution levels. Although studies will often aim to improve daylight distribution inside the occupied space (Doulos *et al.*, 2008; Freewan, 2010), these rely on the calculation of a uniformity criterion.

There are several methods of calculating the uniformity of daylight distribution on the horizontal work surface. The aim of uniformity criteria is to ensure illumination is distributed evenly across the space (Littlefair *et al.*, 1994). Although furniture is usually not considered in the analysis and uniformity calculations only take the daylight received at the horizontal surface at a predefined height from the floor (Ryckaert *et al.*, 2010), the IES-LM-83-12 (Daylight Metrics Committee, 2012) method recommends that furniture that is at least 0.91 m in height should be included.

The scientific literature contains many methods of describing daylight distribution and there are many widely accepted approaches used to measure uniformity (Lynes, 1979). One such method of measuring daylight distribution that is recommended by the Society of Light and Lighting is to calculate the uniformity criterion by dividing the minimum and maximum illuminances found on the horizontal work surface (SLL, 2012). It has also been suggested

https://doi.org/10.1080/19401493.2019.1711456
https://escholarship.org/uc/item/04x6v86j

that uniformity can also be calculated from the minimum to average illuminance ratio (Bean, 1975; Constantatos, 1982). The code for interior lighting (CIBSE, 1994) suggests both approaches of calculating uniformity. When it is believed that uniformity may be difficult to achieve, then the minimum to average illuminance should be the preferred criterion. However, recommendations of what is considered to be appropriate levels of uniformity (i.e., 0.5-0.7) are originally based on a study in an artificially lit room masked from the influence of daylight (Slater and Boyce, 1990). Uniformity based on the same ratios may also be calculated with the room's equivalent Daylight Factors under an overcast sky (Lynes, 1979). However, caution over the results has been advised since under any other sky condition, daylight uniformity will significantly worsen compared to an overcast sky (Dewey and Littlefair, 1998). These criteria of calculating uniformity are generally defined as extreme value based. Yao *et al.* (Yao *et al.*, 2017) suggests there are two alternative methods of estimating uniformity, namely, statistical and pattern based.

Mathieu (Mathieu, 1989) proposed the statistical uniformity (SU) that is calculated according to (1). This makes use of the standard deviation (σ) and average mean illuminances ($\bar{Ex}$) on the horizontal plane. The author showed that the SU does not vary when the size of the analysis grid changes but does when the minimum to average illuminance ratio was used. Another similar proposal by Armstrong (Armstrong, 1990) divides the mean illuminance by the standard deviation, which gives the criterion called the coefficient of variation (CV). Since these criteria do not rely on extreme illuminances values, they are not influenced by the minima and maxima illuminance values.

$$\mathrm{SU} = \frac{\bar{Ex} + \sigma}{\bar{Ex} - \sigma} \qquad -\infty \leq \mathrm{SU} \leq \infty \text{ and } \mathrm{SU} \in \mathbb{R} \tag{1}$$

The SU criterion can potentially take on a large range of values, which makes it difficult to interpret. A third statistical method of calculating uniformity given by Mahdavi (Mahdavi, 1997) is the uniformity factor (UF), which ranges from values between zero and one (2):

$$\mathrm{UF} = \frac{\bar{Ex}}{\bar{Ex} + \sigma} \qquad 0 \leq \mathrm{UF} \leq 1 \text{ and } \mathrm{UF} \in \mathbb{R} \tag{2}$$

The third criteria group are pattern based. Mahdavi and Pal (Mahdavi and Pal, 1999) argued that a limitation of extreme value and statistical methods is that they cannot be used to estimate uniformity when the horizontal surface contains different spatial patterns (i.e., complex illuminance distributions on the horizontal surface). They proposed an entropy-based index (EBI) that calculated the illuminance distributions from global and local areas of analysis grid. These can be used to calculate the topological illuminance distribution of a target grid area. However, it has been argued that the EDI cannot distinguish visual patterns the same way the human eye can (Wang *et al.*, 2004).

Regardless of the complexity of the uniformity criteria, we believe they provide a limited description of how daylight is distributed in buildings because they need to reduce it to single

https://doi.org/10.1080/19401493.2019.1711456
https://escholarship.org/uc/item/04x6v86j

numerical value. On the horizontal work surface, daylight causes a large variation in illuminance levels (Nicol *et al.*, 2006) and understanding this behaviour, beyond uniformity, is crucially when describing the luminous behaviour of any building (Tregenza, 2017, 1986). This spread in the data is created by a high number of spatial and temporal dimensions that should be fully considered when the daylight distribution is evaluated. Spatial dimensions can be defined by the set number of analysis points used to capture illuminances on the horizontal surface, which can be calculated or specified according to recommended guidelines (BCA Green Mark, 2016; Daylight Metrics Committee, 2012; SLL, 2012). Temporal dimensions are those that vary across the occupied hours. While many studies evaluate daylight under a limited number of conditions (i.e., equinoxes or solstices (e.g., (Canziani *et al.*, 2004; Freewan, 2010; Freewan *et al.*, 2008; Sun *et al.*, 2017; Ullah *et al.*, 2017; Zhu *et al.*, 2018)), there are an enormous number of temporal dimensions (i.e., month, days, hours, etc.). As time varies, there are constant in the sun position, cloud patterns, weather, etc. that can significantly influence the daylight conditions inside any given building (Tregenza, 1999).

However, since there is a large number of dimensions that need to be considered, there are often difficulties interpreting the data or to simplify the problem only specific days and times are considered (solstices, equinox, etc.). Similar observations were reported when luminance distribution patterns were evaluated on the horizontal and vertical plane (Parpairi *et al.*, 2002). Nevertheless, in many scientific domains, the collection of high dimensional datum is not uncommon and researchers will often use dimensional reduction to help interpret their data (Bouveyron *et al.*, 2007). Dimension reduction allows the large number of dimensions to be reduced without losing information contained in the original data (i.e., the variability) (Bouveyron and Brunet-Saumard, 2014).

We think that daylight uniformity should be evaluated by identifying the most representative illuminance distribution patterns on the horizontal plane across the occupied hours of the building. Representative daylight illuminance distribution patterns can be used to describe a large subset of different daylight illuminance distributions that form a statistical relationship with each other across a number of temporal dimensions. Since it is possible that two or more conditions can have the same degree of uniformity – as calculated by available criteria – but different daylight illuminance distributions due to temporal variation, an alternative method is needed to provide a better understanding of daylight performance. We aim to prove that a dimension reduction technique can be used to reduce the large number of spatial illuminance visualisations to a small number of representative patterns.

2. Methodology

Two different building models were used in this study. We created a rectangular ‘shoebox’ model of dimensions 4 x 8 x 2.8 m, with a side-lit opening (Figure 1). This model was used as a scenario to demonstrate our approach. The opening appeared in the south façade of the model with dimensions of 3.74 x 1.39 m and creates a sill depth of 0.06 m. We used the optical properties and the simulation parameters recommendations suggested by the

https://doi.org/10.1080/19401493.2019.1711456
https://escholarship.org/uc/item/04x6v86j

IES LM-83-12 standard (Daylight Metrics Committee, 2012). The internal surface reflectance (τ) properties of the model were, respectively, τ_{floor}= 0.20, τ_{wall}=0.50, $\tau_{sill\ bars}$= 0.35 and $\tau_{ceiling}$= 0.80. We used a window with a visible transmittance of 65 %.

To ensure that the proposed approach can work for a more elaborate design proposal, we repeated our approach when considering a complex building geometry (McCormick et al., 2017). We used a model with multiple windows orientated in different directions (i.e., south and east), horizontal and vertical sill bars, and external overhangs and shading fins (Figure 1). The internal surface reflectance (τ) properties of the model were: τ_{floor}= 0.20, $\tau_{sill\ bars}$= 0.20, τ_{walls}= 0.70, and $\tau_{ceiling}$= 0.70. The visible transmittance of the glazing was 65 %. We considered no exterior obstructions or interior furniture in both models.

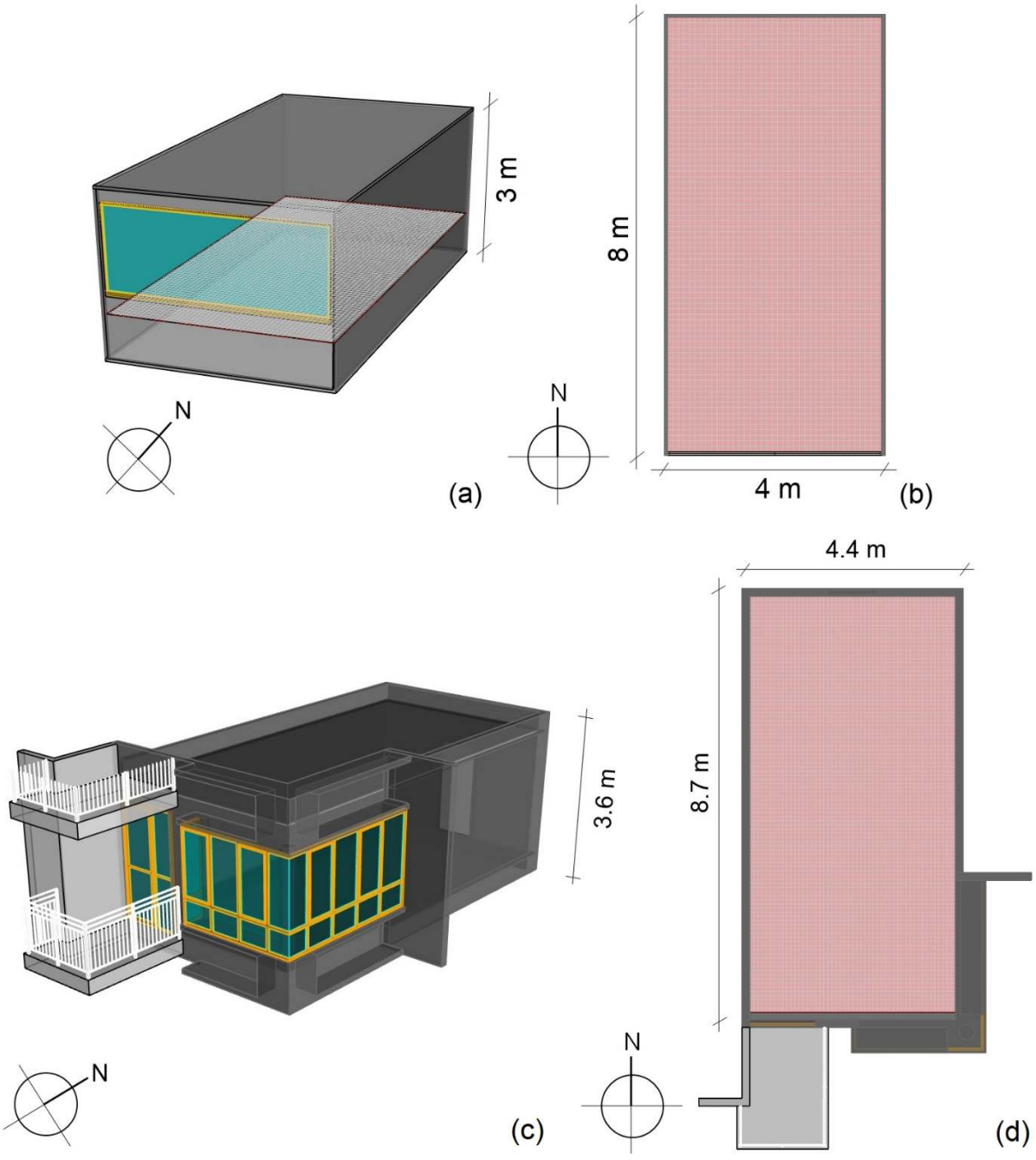

https://doi.org/10.1080/19401493.2019.1711456
https://escholarship.org/uc/item/04x6v86j

Figure 1. Perspective view of the shoebox model as seen from Rhinoceros (a) and top view of the daylight analysis grid used to evaluate illuminance distribution patterns (b). Perspective view of the complex model as seen from Rhinoceros (c) and top view of the daylight analysis grid used to evaluate illuminance distribution patterns (d).

Researchers often evaluate the performance of daylighting systems (i.e. light-shelves, light-pipes, etc.) under different climatic conditions (Kurtay and Esen, 2017; Sun et al., 2017; Tsang et al., 2018), while designers may be interested in how daylight varies according to the available building parameters (i.e., window orientation, glass type, shading strategy, window size, etc.). We repeated our analyses to evaluate the daylight illuminance distributions when: (1) Considering two climates, Singapore (1.35^{o} N) and Oakland, California (38^{o} N) and (2) when three different side-lit orientations were selected (south, east and west, respectively). Simulations were repeated using the same temporal conditions, each time collecting 3200 illuminance data points. Only Singapore was considered in the second analysis.

We performed annual climate-based simulations using the Department of Energy weather data files for Singapore and Oakland, California. We used the occupancy schedule to simulate annual daylight performance metrics in Singapore (BCA Green Mark, 2016), which performs daylight calculations at one hour intervals from 08:00 to 17:00 every day of the week and excludes daylight savings. Although countries have different occupancy schedules for the same building typology, we used a single schedule to provide a direct comparison across the two climates.

To simulate illuminances on a horizontal surface, we used the software DIVA (version 4.1.0.8) for Grasshopper (version 0.9.0076) to perform annual climate daylight analyses on our computer model and then to extract the hourly illuminance data based on the occupancy schedule. This gave us 3285 different temporal conditions. While DIVA is a plug-in for the modelling software Rhinoceros (Jakubiec and

, 2011), Radiance is the simulation engine that uses of method of backwards raytracing to calculate the light levels (Ward and Shakespeare, 1998). We used the following Radiance simulation parameters: Ambient bounces= 7, ambient divisions= 4096, ambient resolution= 512, ambient super-samples= 1 024, ambient accuracy= 0.1, and limit weight= 0.001. No artificial lighting was considered.

For both models considered (Figure 1), we used an illuminance grid spacing between each node of 0.1 m, giving a higher resolution of daylight distribution than recommended standards (BCA Green Mark, 2016; Daylight Metrics Committee, 2012). The simulation grid was the area of the model floor and was elevated to a distance of 0.75 m to act as the working desk surface. When testing other grid size spaces (e.g., 0.3 m and 0.6 m) this produced similar findings when applying our analysis.

2.1. Principal components analysis

Principal Components Analysis (PCA) was used to reduce a large number of correlated variables (i.e., dimensions) into smaller linearly related components, which are strongly

https://doi.org/10.1080/19401493.2019.1711456
https://escholarship.org/uc/item/04x6v86j

correlated with each other (Field, 2013). The components would give a compact description of the original data (Liang *et al.*, 2002), thereby allowing complex high dimensional data to be more easily interpreted (Lever *et al.*, 2017). In our study, the principal components are groups of daylight illuminance distributions from different temporal conditions which are linear related to each other. Each principal component is independent from others and are derived from important simulation parameters (i.e., the building model dimensions and properties, time conditions, and climate data).

PCA has many applications in different fields of engineering research including lighting (Nayar and Murase, 1994). Ramamoorthi (Ramamoorthi, 2002) use PCA to evaluate light variability on a set of images that were exposed to different conditions. He showed that light variability could be explained with five components and this explained up to 96 % of the variance from high-dimensional data with large variations in illumination. Lee *et al.* (Lee *et al.*, 2005) showed that PCA could be used to analyse a large set of images under a wide of lighting conditions to be used for facial recognition. Zhao and Yang (Zhao and Yang, 1999) showed how a PCA could be used to account for changes in the light source type, its intensity, photometric properties, and reflections both diffusive and specular.

We used PCA to determine how much illuminance variability can be explained when the total amount of variance in the data is reduced into a smaller number of linearly separable components. We created a Python script to export the annual illuminance values from Grasshopper to a comma-separated file using a data format which was ready to be analysed. The formatting organised the temporal conditions into 3285 columns (i.e., nine hourly time-steps each day multiplied by the 365 days during the year), and each column contained rows of illuminance data from the individual grid sensors. To perform a PCA, we used the 'prcomp' package for the software R (version 3.4.4) (Hothorn and Everitt, 2009).

Common to most methods of PCA are processes of centring and scaling. Centring is performed by subtracting the arithmetic mean average of all illuminances for each scenario with each of its individual illuminances, which are then plotted linearly as a vector that is centred on a value of zero (Smith, 2002). Since scenarios with higher variances will naturally explain more variability in the data, PCA will also apply scaling. Since the spread in our data (i.e., the distribution of the illuminance points across the different temporal conditions) may not be equal, scaling attempts to normalise the original variables by plotting them onto a new scale of a constant length (Wentzell and Hou, 2012).

To derive the most representative illuminance distribution for each principal component, we used the temporal condition containing the highest correlation coefficient. Since the correlation coefficients are standardised values (Jolliffe and Cadima, 2016), they directly compare the strength of the relationship across two or more temporal conditions. Hence, we used the illuminance distribution that had the highest degree of correlation with all other daylight patterns from the temporal conditions that loaded into the same principal component. By utilising this method to derive the representative daylight distributions, this allows designers to relate the results of the PCA back to the original illuminance data.

https://doi.org/10.1080/19401493.2019.1711456
https://escholarship.org/uc/item/04x6v86j

3. Results

3.1. Correlation approach

At the basis of our approach, we assume that at each individual illuminance grid point is statistically related with the same grid point at a different time. When generalising this to all grid points across two conditions, the illuminances would be correlated. To show this, we plotted three conditions against each other using the shoebox model. We used 09.00 on the 21st January as the reference condition, and 09.00 on 21st February and June as comparative cases. Simulations were ran at each of these conditions and the 3200 illuminance points were plotted against each other in Figure 2.

To show this, we plotted three conditions against each other. We used 09.00 on the 21st January as the reference condition, and 09.00 on 21st February and June as comparative cases. Simulations were ran at each of these conditions and the 3200 illuminance points were plotted against each other in Figure 2. The sky conditions described in the EnergyPlus weather file for Singapore and the temporal conditions were, respectively, predominantly clear on January 21st at 09:00 and partially covered by clouds or other obscuring phenomena in the sky (e.g. fog, mist or smoke) on February and June 21st at 09:00.

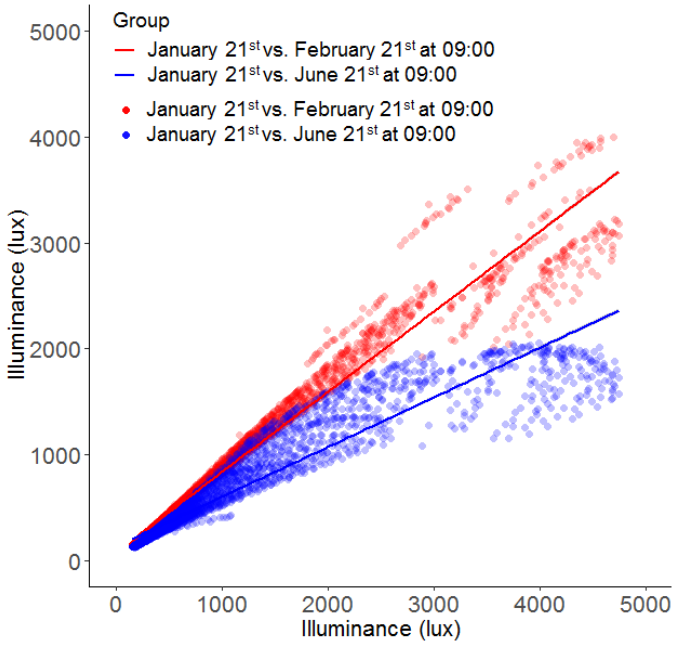

Figure 2. Graphs to show the comparison between the 3200 illuminance sensors across two conditions in Singapore: (blue) 09.00 21st January vs. 09.00 21st June and (red) 09.00 21st January vs. 09.00 21st February.

The figure plots generally show linear relationships. We also produced several matrix scatters plots – selecting several random scenarios – to determine whether the assumption of

https://doi.org/10.1080/19401493.2019.1711456
https://escholarship.org/uc/item/04x6v86j

linearity had been met in other cases. We used the Pearson's correlation coefficient, r to measure the strength of association between the variables plotted in the figures.

High correlation coefficients were found for comparisons between January and June and January and February (r= 0.94 and r= 0.96, respectively). This shows that in both cases, the illuminances on the same grid points measured are linearly correlated with each other at different time intervals. The correlation coefficients – when expressed as the proportion of variance explained (r^2) – can be used to show that 88 % (0.94^2 x 100) and 92 % (0.96^2 x 100) of the variability in illuminance is determined by the linear relationship between the two variables. Although the illuminances across the two conditions are strongly correlated to each other, the slope of the linear regression lines are different. This suggests that there are different illuminance distribution patterns on the horizontal surface.

3.2. Global horizontal illuminances

To help interpret the PCA, we plot the global horizontal illuminance data found in the EnergyPlus weather files for Singapore and Oakland, California. Figure 3 shows the mean average global horizontal illuminance values (i.e., total direct and diffused daylight received on a horizontal surface) for each month. As expected, the cumulative illuminance values for Singapore remain relatively constant across the year due to its close proximity to the equator. For Oakland, California, the illuminance values vary considerably more, whereby the lowest mean illuminances occur around December and peak in June. This indicates that daylight levels vary more across the year in Oakland, California compared to the variability in illuminances in Singapore.

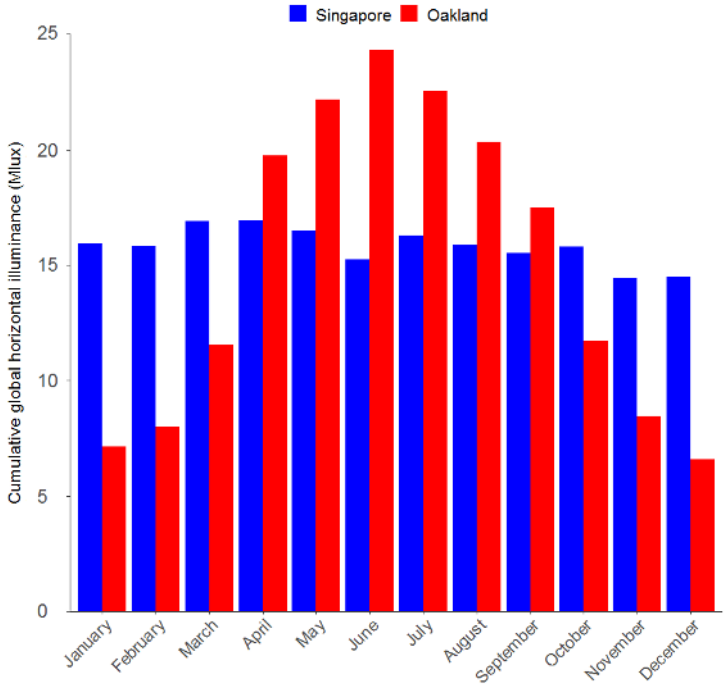

Figure 3. Cumulative plots showing the global horizontal illuminance (total direct and diffused) received on a horizontal surface in Oakland, California and Singapore. Note: the illuminances are expressed in Mega-lux.

https://doi.org/10.1080/19401493.2019.1711456
https://escholarship.org/uc/item/04x6v86j

3.3. Representative spatial daylight distributions: Shoebox model

Table 1 presents, the proportion of variance and cumulative variance each component can explain according to the first six components extracted from our PCA for both Singapore and Oakland California. Since Singapore is located near the equator, there is less annual variability in daylight levels compared to Oakland California. We anticipated that few components would have been needed to explain the annual variability in illuminance distribution on the horizontal surface. In fact, the cumulative variance for principal component 1 in Singapore could explain the same amount of variability as the cumulative variance from the first five principal components for Oakland, California. When considering the cumulative variance explained for two principal components in Singapore, more principal components – than those displayed in Table 1 – would be needed to arrive at the same amount of variance that can be explained for Oakland, California.

Table 1. Proportion and cumulative variance that can be explained for each component for Singapore and Oakland, California.

Component	**Singapore**		**Oakland, California**	
	Proportion of variance explained (%)	*Cumulative variance explained (%)*	*Proportion of variance explained (%)*	*Cumulative variance explained (%)*
1	93	93	61	61
2	3	96	17	78
3	3	99	8	86
4	0	99	5	90
5	0	99	3	93
6	0	99	1	94

https://doi.org/10.1080/19401493.2019.1711456
https://escholarship.org/uc/item/04x6v86j

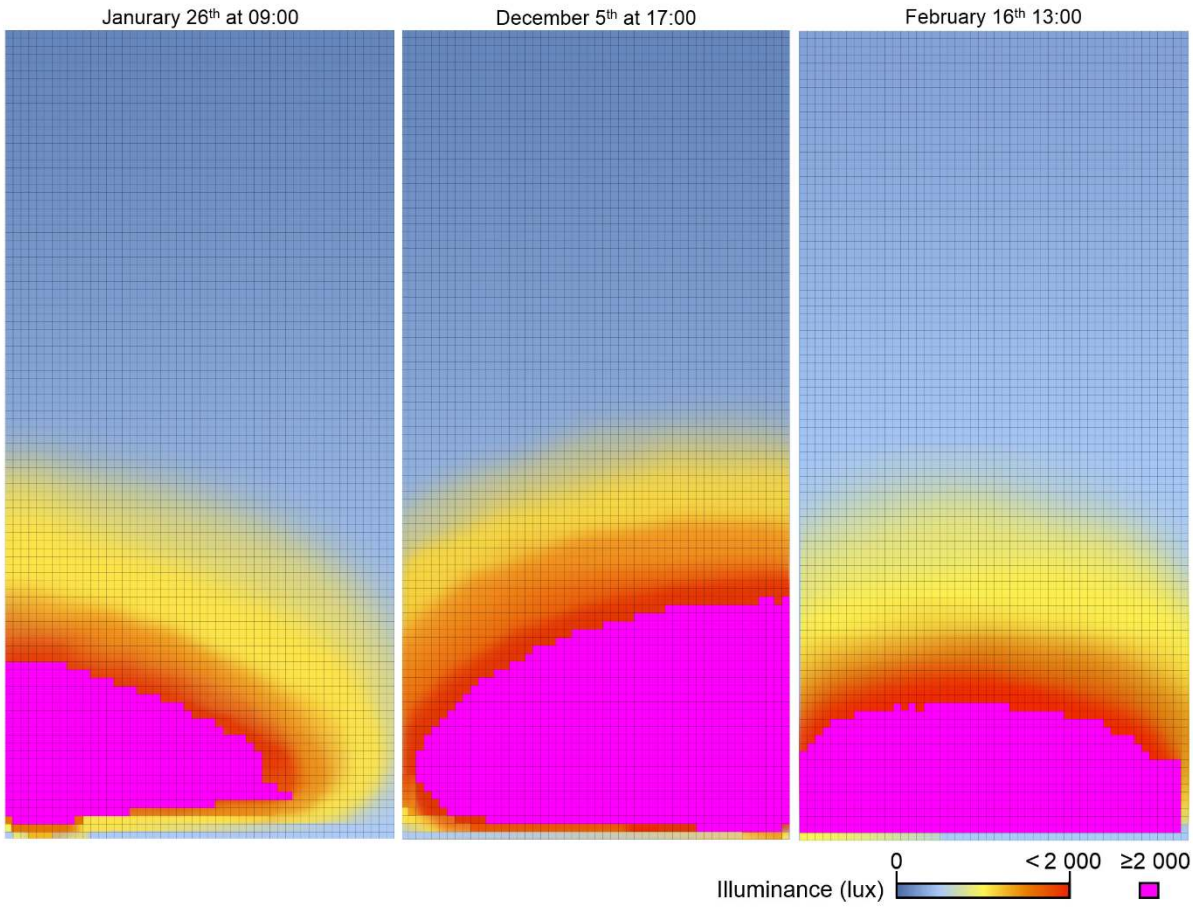

Figure 4. The representative illuminance distributions derived from the PCA in Singapore. Principal component 1: January 26th at 09:00 (*left*), component 2: December 5th at 17:00 (*centre*), and component 3: February 16th at 13:00 (*right*).

The distributions shown in Figure 4 display the three principal components that are highly correlated to a larger group of daylight patterns, which represent 99 % of the illuminance variability (Table 1). While there are a range of illuminance conditions throughout the year, our approach identifies some of the most typical temporal and spatial daylighting conditions for designers to review. To compare the representative daylight distributions that were derived from the PCA (Figure 4) with existing uniformity criteria, we calculated the minima, maxima, mean averages and standard deviations of the illuminances, different illuminance ratios, the SU, CV, and UF (Table 2).

Table 2. Summary of uniformity criteria used to describe the representative illuminance distributions (as presented in Figure 4) for Singapore.

Component	**One**	**Two**	**Three**
Loading: Month/day and time	*01/26 at 09:00*	*12/05 at 17:00*	*02/16 at 13:00*
Minimum illuminance (lux)	160	256	232
Maximum illuminance (lux)	4392	9400	33300
Mean average illuminance (lux)	689	1898	2020
Standard deviation (lux)	690	2455	5405

https://doi.org/10.1080/19401493.2019.1711456
https://escholarship.org/uc/item/04x6v86j

Minimum to maximum ratio	0.04	0.03	0.01
Minimum to average ratio	0.23	0.13	0.11
SU	-1379	-7.81	-2.19
CV	1.00	0.77	0.38
UF	0.50	0.44	0.27

The three representative daylight distributions occurred at different times of the day: Morning (component 1), evening (component 2), and afternoon (component 3). We anticipated this finding as there is little seasonal variability in Singapore due to its close proximity to the equator. Notably, the date and months of the three principal components do not coincide with the annual equinoxes or solstices. This is a clear indication that the common practice of using these days are not representative of a wider range of annual daylight distributions. The uniformity criteria for each of the three components show differences in the distribution of daylight on the horizontal surface. Specifically, that there are decreasing levels of uniformity from principal component 1 to 3. Although this suggests that uniformity criteria can distinguish different daylight distributions, we repeated the same evaluations for Oakland, California to test the same uniformity criteria in another climate that has more seasonal variability.

To illustrate the representative illuminance distributions from each principal component in Oakland, we again used the temporal conditions with the highest correlation coefficients from each component (Figure 5). Unlike the illuminance distributions in Singapore, the daylight levels in Oakland are much more dependent on seasonal variability. These can be seen in the figure images as higher daylight levels reach deeper into the room from the side-lit opening. Although this created more illuminance variability on the horizontal plane, PCA explained 94 % of the variance in our data from six principal components.

https://doi.org/10.1080/19401493.2019.1711456
https://escholarship.org/uc/item/04x6v86j

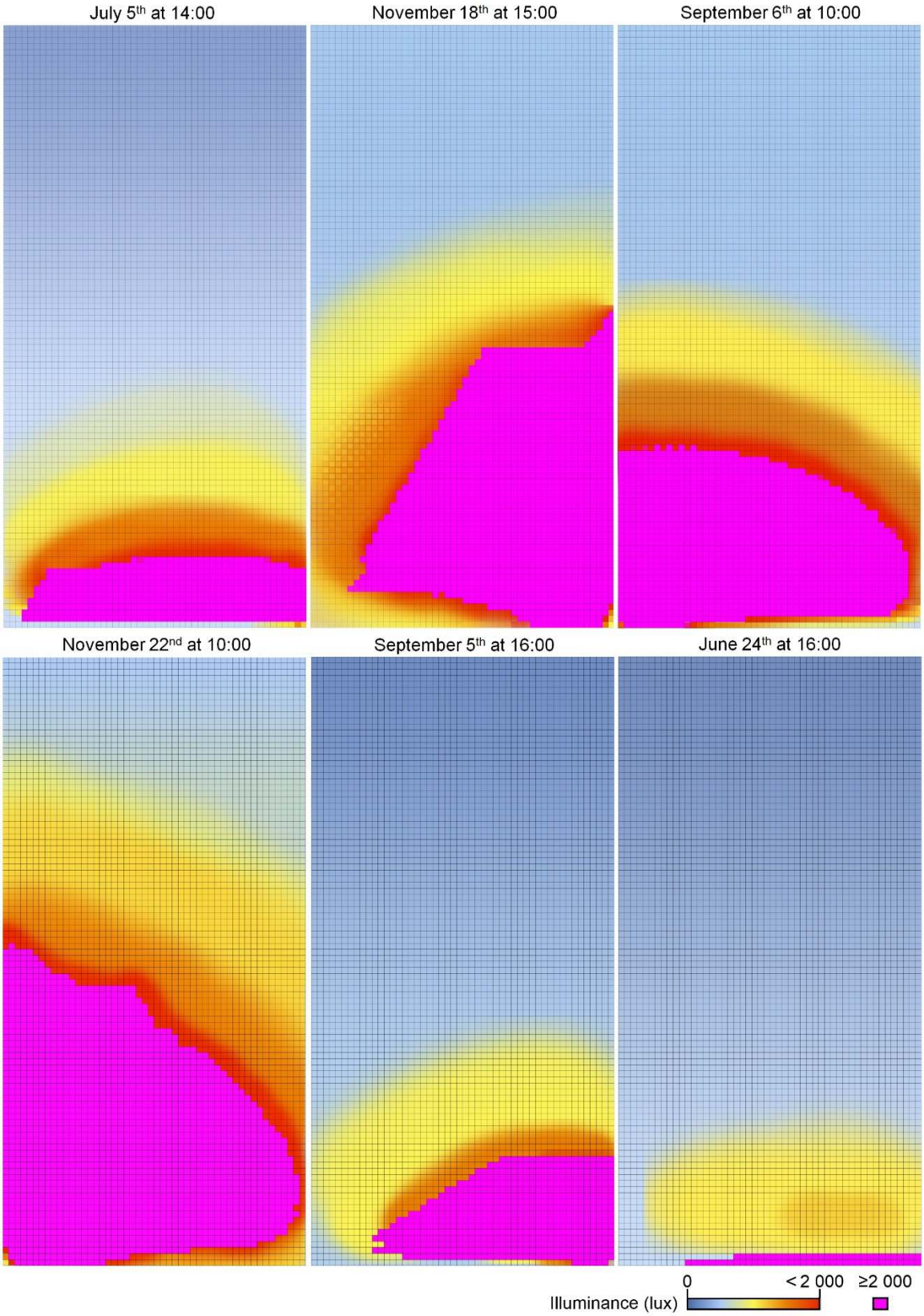

Figure 5. The representative illuminance distributions derived from the PCA in Oakland California. Principal component 1: July 5th at 14:00 (*top-left*), component 2: November 18th at 15:00 (*top-centre*), component 3: September 6th at 10:00 (*top-right*), component 4: November

https://doi.org/10.1080/19401493.2019.1711456
https://escholarship.org/uc/item/04x6v86j

22nd at 10:00 (*bottom-left*), component 5: September 5th at 16:00 (*bottom-centre*), and component 6: June 24th at 16:00 (*bottom-right*).

In Table 3 we report the uniformity levels describing the daylight distribution using existing criteria for the illuminances presented in Figure 5. Generally, the extrema-based criteria show similar values in uniformity across the six principal components meaning that they are not able to distinguish between different conditions. The uniformity criteria could not differentiate between the representative daylight distributions (i.e., the principal components in Table 3). The extreme value based criteria (i.e., minimum to maximum and minimum to average ratios) generally show similar values of uniformity for principal components 1, 2, 3 and 5. The statistical based criteria (i.e. SU, CV and UF) show relatively similar values for principal components 1, 3 and 5. Comparing these values for the principal components to the visualisations shown in Figure 5 reveals that the daylight distributions are in fact significantly different for each of the representative conditions. Therefore, our results show that existing uniformity criteria provide a poor evaluation of daylight distribution.

Table 3. Summary of uniformity criteria used to describe the representative illuminance distributions (as presented in Figure 5) for Oakland, California.

Component	**One**	**Two**	**Three**	**Four**	**Five**	**Six**
Loading: Month/day	*07/05*	*11/18*	*09/06*	*11/22*	*09/05*	*06/24*
Loading: Time	*14:00*	*15:00*	*10:00*	*10:00*	*16:00*	*16:00*
Minimum illuminance (lux)	200	544	280	240	810	132
Maximum illuminance (lux)	29216	27228	28976	5664	22520	5424
Mean average illuminance (lux)	1767	5233	2370	1245	2178	500
Standard deviation (lux)	4985	7652	4968	1306	4283	696
Minimum to maximum ratio	0.01	0.02	0.01	0.04	0.01	0.02
Minimum to average ratio	0.11	0.10	0.12	0.19	0.08	0.26
SU	-2.10	-5.33	-2.82	-42	-3.07	-6.08
CV	0.35	0.68	0.48	0.95	0.51	0.72
UF	0.26	0.41	0.32	0.49	0.34	0.42

To determine how well the daylight distributions represented each principal component, we plot 150 temporal conditions for each climate on a scatter plot matrix using the Pearson's correlation coefficient, r (Figure 6). This plots the first 50 temporal conditions that load into each of the first three principal components against each other for both Singapore (a) and Oakland, California (b). Figure 6 shows that within each principal component, the temporal conditions (including the representative case) generally have a very strong degree of association with each other ($r \geq 0.90$). When comparing the correlation coefficients across the principal components, a much lower degree of association can be found (i.e., they are independent from each other). Although we only include the first 50 temporal conditions for each principal component to demonstrate the relationships, it is important to highlight that

https://doi.org/10.1080/19401493.2019.1711456
https://escholarship.org/uc/item/04x6v86j

many more temporal conditions load into the principal components with high correlation coefficients. Nevertheless, this shows that the representative distributions identified can be generalized across the other temporal conditions found in the same principal component.

Since Figure 6 can only be used to visualize the first 50 temporal conditions that load into the first three components for each climate, it is important to understand the relationship of the representative daylight distributions with all other scenarios that were considered. If some cases selected do not represent the principal component well, some important daylight distributions may not be evaluated.

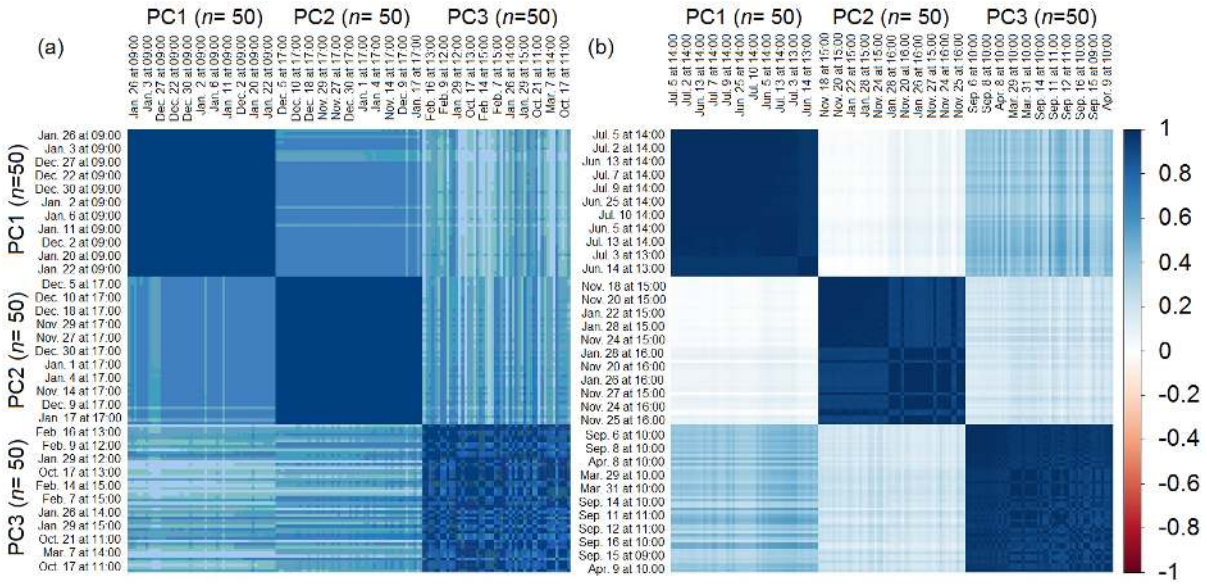

Figure 6. Scatterplot matrix showing the Pearson's correlation coefficients, *r* for the first 50 temporal conditions that load into the first three principal components for Singapore (a) and Oakland, California (b).

Table 4 presents the correlation coefficients, *r* for the 3285 temporal conditions considered, which are organized according to their degree of association with each principal component. To interpret the outcome we used the recommendations given by Ferguson (Ferguson, 2009), whereby thresholds for "small", "moderate" and "large" ($r \geq 0.20$, 0.50 and 0.80, respectively) are given.

Table 4. Cumulative number of temporal conditions that load into the first three principal components for the two climates: Singapore and Oakland, California. The loadings are organized according to their degree of association with the principal component based on the threshold of "small", "moderate" and "large", respectively.

Correlation coefficients, *r*	**Principal components: Singapore**			**Principal components: Oakland**		
	1	*2*	*3*	*1*	*2*	*3*
Strong ($r \geq 0.70$)	1000	886	234	598	508	301
Moderate ($0.50 \leq r < 0.70$)	1629	1689	549	442	609	920

https://doi.org/10.1080/19401493.2019.1711456
https://escholarship.org/uc/item/04x6v86j

Small ($0.20 \leq r < 0.50$)	599	666	2501	989	1016	1216
Negligible ($r < 0.20$)	57	44	1	1256	1152	848

When more temporal conditions have a "strong" associations, this shows that the representative daylight distribution selected will provide a better representation of the principal component. In other words, there is a higher degree of similarity between the distribution of the representative case with other temporal conditions that have strong correlation coefficients. This degree of similarity decreases when the correlation coefficients in the same principal component also decrease. Because Singapore generally contains more temporal conditions that have correlations of a "moderate" or "strong" magnitude, we are able to determine that the first three representative daylight distributions represent the principal components and the data better than those for Oakland, California. To minimise the risk of excluding important daylight distributions in the data, more principal components should be evaluated for Oakland, California.

3.4. Principal Component Analysis plots

We plot the illuminance data using new scaled axes (Figure 7). The x-axis shows the scale belonging to principal component 1 and the y-axis corresponding to principal component 2. This type of plot allows two important aspects to be visualised when varying the location and window orientation for the first two principal components: (1) the direction in which the maximum variation in the data (i.e. the eigenvectors) can be explained when considering the 3658 daylight illuminances distributions; and (2) the amount of variance that can be explained (i.e. the eigenvalues). Regardless of the sign of the values (i.e. positive or negative), the x- and y-axes are the unit-less eigenvectors and show the magnitude of variance that can be explained in a certain direction by the principal components.

We used a 95 % confidence interval to draw two ellipses to mark the position of the data points belonging to either group (i.e. Singapore or Oakland, California) across the principal components. These utilise the data points to construct an ellipse based on the mean average of their distributed within a confidence level of 95 %. Because the ellipses demarcate the location of the groups, they show how much variability can be explained along each axis (Husson *et al.*, 2005). While PCA will scale the illuminances of the temporal cases from each climate so that they are approximately equal, we found that the range in illuminances across the two conditions were still different. To help ensure the variances are more equally spread across the variable length for both climates, we used a common procedure to PCA, which is to logarithmically transformed the data (Baxter, 1995). In both figure plots, the illuminance values are centred about zero and have been scaled so that data for each group variable have variances that are of approximately equal length.

Since Oakland, California naturally has more variation in daylight levels due to seasonal variability, there is a larger spread in the data points and as a result, more variance in the data can be explained by principal component 2 (i.e., the length of the ellipse is larger across the y-axis than for Singapore (Figure 7(a))). In fact, 17 % of the variability can be explained by

https://doi.org/10.1080/19401493.2019.1711456
https://escholarship.org/uc/item/04x6v86j

principal component 2 in Oakland, California (see Table 1) and only 3 % in Singapore. However, not all the data points for Oakland, California are captured by principal components 1 and 2. Hence, more principal components are needed to capture additional variability that remains within the data.

While the general shape of the illuminance data points for each climate are relatively similar (Figure 7(a)), this was to be expected since we used the same physical geometry for our model. Another aspect to consider is how daylight distribution for the same climate will vary when changing a physical parameter (Figure 7(b)). Along the y-axis (principal component 2), the eigenvalues for the west window orientation are positive, but are negative for the east window orientation. For the southern window orientation, the values are a mixture of both positive and negative. To help interpret the eigenvectors in Figure 7 plot (b), we evaluated the correlation coefficients for the 3658 temporal conditions when considering the first two principal components and the three different window orientations (i.e., how well a daylight illuminance distribution for one temporal condition correlates with all others in the same principal component). The strongest relationships occur at different times during the occupancy schedule in Singapore. For the east orientated window these generally occur at midday (principal component 1) and early morning (principal component 2), for the west orientated window in the late afternoon (principal component 1) and early afternoon (principal component 2), and for the south orientated window in the early morning (principal component 1) and late afternoon (principal component 2). While the temporal condition with the strongest correlation coefficient was used as the representative daylight illuminance distribution for each principal component, similar temporal conditions found in the same principal component also share a strong statistical relationship with each other.

Although the same data is used in Figure 7 plot (a) for Singapore and (b) for the southern window orientation, the eigenvalues are not the same. This is largely due to the fact that the PCA takes into account the direction in which the maximum variance can be explained when also considering the other group variables and how these relate to the data from the southern window orientation in Singapore.

https://doi.org/10.1080/19401493.2019.1711456
https://escholarship.org/uc/item/04x6v86j

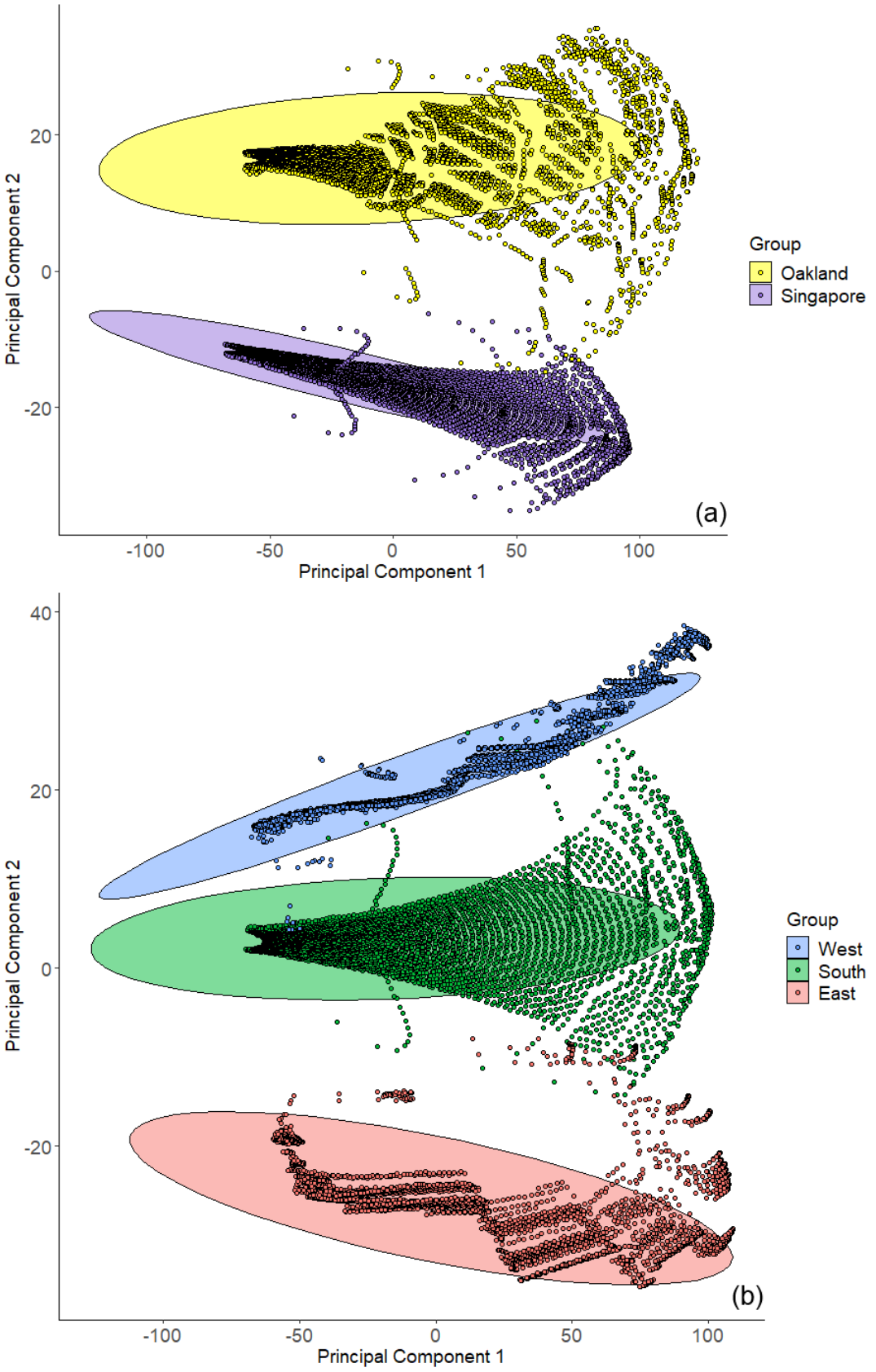

Figure 7. Plot to show principal component 1 and principal component 2 when they are categorized by a grouping variable: (a) according to our two locations: Singapore and

https://doi.org/10.1080/19401493.2019.1711456
https://escholarship.org/uc/item/04x6v86j

Oakland, California and (b) according to three window orientations: South, east and west in Singapore.

We believe the PCA plots allow others to gain more insights into the daylight performance of their building proposal. Because the plots directly compare two or more groups, they are also able to show how much variability there is in the annual daylight illuminance distributions for each for each condition (e.g. location or window orientation). We believe the plots can also be used to help improve annual daylight illuminance uniformity, which could be used to prevent daylight glare and ensure adequate levels of room lighting. For example, plot (a) shows that Singapore has less variability in the daylight illuminance distributions when using the same occupancy schedule. While this different occurs because of difference in the location, a designer may want to install a daylighting strategy to minimize the spread in the data points for Oakland, California. With less variability present in the data, fewer representative illuminance distributions would be needed to understand the annual performance of daylight inside the space.

3.5. Representative spatial daylight distributions: Complex model

Of the 3285 variables considered, PCA could explain 98 % of the illuminance variability with six principal components in Singapore and 88 % in Oakland, California (Table 5). The results our similar to our initial analyses (Table 1), which also shows that more variability can be explained in Singapore with few principal components when the same model is evaluated. More principal components would be needed for Oakland, California.

Table 5. Proportion and cumulative variance that can be explained for each component for our alternative model in Singapore and Oakland, California.

Component	**Singapore**		**Oakland, California**	
	Proportion of variance explained (%)	*Cumulative variance explained (%)*	*Proportion of variance explained (%)*	*Cumulative variance explained (%)*
1	83	83	67	67
2	10	93	8	76
3	2	95	5	81
4	1	96	3	84
5	1	97	2	86
6	1	98	2	88

When evaluating the representative daylight distributions for the first two principal components in Singapore (Table 5), these occurred on: 30th May at 15:00 (component 1) and 2nd February at 10:00 (component 2). The two principal components can explain 93 % of the annual variability in illuminance on the horizontal surface for our alternative model used. For Oakland, California, the first two principal components occurred on: 9th December at 10:00

https://doi.org/10.1080/19401493.2019.1711456
https://escholarship.org/uc/item/04x6v86j

(component 1) and 19th April at 13:00, respectively. These were based on the temporal conditions that had the highest correlation coefficients for each principal component.

From these further analyses using an the building shown in Figure 1, the findings show that our approach can still be applied when adding more complexity to the daylight simulation. Therefore, we believe that the PCA approach can be applied more widely for any given design proposal to obtain the representative daylight illuminance distributions.

Although it is difficult to directly compare our approach to what would otherwise be used in common practice, we compared the illuminance distribution indicators from the solstices and spring equinox at three-hour intervals to those calculated from the first three principal components for the complex model in Oakland, California (Table 6).

Depending on which criteria of daylight performance is selected, the interpretation given would vary considerably. However, the same criterion provides a relatively similar description of how the daylight performs across both approaches (i.e., common practice and PCA). For example, the minimum to maximum ratio generally shows that daylight illuminance is widely distributed across the horizontal surface of the room, while the minimum to average ratio shows that there is a higher degree of daylight uniformity in the same space. The statistical based criteria (i.e., SU, CV and UF) also show relatively similar values across both approaches. While it needs to be acknowledged that these criteria may not necessarily provide a good indicator of daylight distribution, our approach may give results that are comparable to common design practice. However, our approach also gives the designer additional information. From these three distributions, they would know that they are evaluating 81 % of the total annual variability caused by daylight.

Table 6. Summary of uniformity criteria used to describe the illuminance distributions based on common practice (i.e., spring equinox and the solstices and at 09:00, 12:00 and 15:00) and for the first three principal components based on our approach for Oakland, California.

Common practice									
Loading: Month/day	*03/21 (spring equinox)*			*06/21 (summer solstice)*			*12/21 (winter solstice)*		
Loading: Time	*09:00*	*12:00*	*15:00*	*09:00*	*12:00*	*15:00*	*09:00*	*12:00*	*15:00*
Minimum illuminance (lux)	253	192	120	189	157	113	415	275	114
Maximum illuminance (lux)	17933	26065	1306	24719	1894	1066	9934	16547	10330
Mean average illuminance (lux)	3370	1752	406	2628	603	388	2653	3406	483
Standard deviation (lux)	5750	5051	283	6469	438	250	2535	5798	973
Minimum to maximum ratio	0.01	0.01	0.09	0.01	0.08	0.11	0.04	0.02	0.01
Minimum to average ratio	0.08	0.11	0.30	0.07	0.26	0.29	0.16	0.08	0.24
SU	-4	-2	-6	-2	6	5	44	-4	-3
CV	0.59	0.35	1.44	0.41	1.38	1.55	1.05	0.59	0.50
UF	0.37	0.26	0.59	0.29	0.58	0.61	0.51	0.37	0.33
PCA approach									
Component	**One**			**Two**			**Three**		

https://doi.org/10.1080/19401493.2019.1711456
https://escholarship.org/uc/item/04x6v86j

Loading: Month/day	*12/09*	*04/19*	*08/01*
Loading: Time	*10:00*	*13:00*	*11:00*
Minimum illuminance (lux)	260	204	264
Maximum illuminance (lux)	5192	30248	20944
Mean average illuminance (lux)	1556	1105	1816
Standard deviation (lux)	1125	3012	3393
Minimum to maximum ratio	0.05	0.01	0.01
Minimum to average ratio	0.17	0.18	0.14
SU	6.22	-2.16	-3.30
CV	1.38	0.37	0.54
UF	0.58	0.27	0.35

While we defined common practice by the nine daylight distributions derived from a clear sky condition (Table 6), the LEED ver.4 daylight credit option 2 specifies a more limited scope of temporal scenarios for designers to evaluate. The United States Green Building Council recommend that illuminance calculations are performed at 09:00 and 15:00 that are within 15 days of the spring or autumn equinox, which represent the clearest sky condition (USGBC, 2019). Alternatively, our approach shows the designer the daylight distributions that should be evaluated, which considers a much wider range of temporal and sky conditions that are contained within the climate weather file. Lastly. Using only three principal components (i.e., daylight distributions), our approach arrived at the same conclusions a designer would have using nine. The proposed dimensionality reduction method is able to select the most representative visualizations, this may lead to better daylighting analysis and design.

4. Discussion

We present here a novel method to evaluate spatial daylight illuminance distributions on the horizontal work surface using PCA. Our findings show that daylight illuminance distributions from 3285 different hourly occupied intervals can be reduced into a smaller number of representative cases. We used two climates (i.e., Singapore and Oakland, California) and two building models of varying complexity to show how this works. Our approach was able to reduce 3285 temporal conditions into a much smaller number (usually less than six) of representative daylight visualizations, while explaining an high degree of annual illuminance variability (usually more than 90 %).

One aspect of this work that may need further consideration would be the number of representative daylight distributions to retain for further evaluation. While the analysis shows how much illuminance variability can be explained on the horizontal surface, it does not provide much indication of how much is an acceptable level. Based on our work, we have provided some recommendations to help others interpret their own work when using PCA.

https://doi.org/10.1080/19401493.2019.1711456
https://escholarship.org/uc/item/04x6v86j

When using a simple model (i.e., Figure 1) and less seasonal variation (i.e., a Singaporean climate), we recommend that at least 95 % of the illuminance variability should be explained by the principal components. When considering a complex geometry (Figure 1) and more seasonal variation (i.e., a Californian climate), we recommend that at least 90 % of the illuminance variability should be explained by PCA. The basis of these thresholds are derived from Table 1 (Singapore) and Table 3 (Oakland, California). Nevertheless, some further interpretation may still be needed by the designer to ensure enough representative distributions are retained to explain the variability in daylight.

Our results also show that while two principal components may have the same degree of uniformity – as calculated by recommended criteria, the daylight distribution inside the room can significantly vary. This was apparent when we tested uniformity criteria for different representative daylight distributions in Oakland, California (Figure 5, Table 3). However, because Singapore required a smaller number of principal components to explain the same amount of illuminance variability (Figure 4, Table 1), it is less likely that uniformity criteria would have given the same values from a smaller number of cases considered. This finding raises some important questions to whether uniformity criteria should be used to evaluate daylight illuminance distributions on the horizontal surface. Studies that have used uniformity criteria to obtain energy savings from daylight responsive sensors (i.e. (Doulos *et al.*, 2008)), may find that their design strategy is not operating at an optimal level of performance.

We believe our approach in daylighting practice has many applications, for example: (1) Following climate-based simulations used to evaluate annual metrics (i.e., daylight autonomy, useful daylight illuminance, etc.), designers may then run simulations targeting specific periods during the year. Typically, standardised point-in-time simulations (i.e., equinoxes and solstices at predetermined hourly intervals) would be applied across any given design proposal. Our approach gives the designer more representative time periods to evaluate, which are based on the climate, physical geometry, and other related parameters that may influence the distribution of daylight. (2) Time-dependent design strategies (i.e., light-pipes or light-shelves) are typically evaluated using uniformity criteria. Our findings show these can provide misleading results and designers need an alternative approach to counter such problems. By extracting the representative daylight distributions, designers can carefully evaluate the illuminance data and visualisations to make more informed decisions. (3) PCA plots allows daylight distribution from more than one proposal to be directly compared (Figure 7). This may also be useful when comparing multiple analysis grids. For example, several grids placed in the same room (i.e., different desk surfaces), the same building (i.e., several rooms with different orientations on different floors), or when introducing shading devices.

We think that the proposed dimensionality reduction method using PCA should be added within DIVA and Grasshopper, whereby illuminance data can be easily produced and readily evaluated. This will automatically generate the representative daylight distributions for the users, which they can interpret alongside the PCA analysis. Following the completion of the

annual simulation, it is also important to highlight that our approach requires a relatively short period of time to derive the representative daylight distributions (i.e., minutes based on the models used in our article).

5. Conclusions

We used principal component analysis to find the most representative spatial daylight distribution patterns. Our new approached showed that we were able to reduce a larger number of illuminance distributions into a smaller of representative patterns. To assess this dimensionality reduction approach, we evaluated climate-based hourly illuminance intervals across a 08:00 to 17:00 occupied schedule to describe the performance of 3285 daylight illuminance distributions on the horizontal surface using climate data for Singapore and Oakland, California. We showed that this approach can be used to help designers and researchers to drastically reduce the number daylight illuminance distributions to be analysed.

Our findings have also shown that existing uniformity criteria do not provide an informative description of how daylight is distributed on the horizontal surface. Although uniformity criteria can show how evenly daylight is distributed across the horizontal surface, they cannot distinguish that one illuminance distribution is significantly different from another. We think further research may be needed to evaluate how the use of these uniformity criteria influence the performance of daylight dimming sensors.

Funding

This work was supported by the Republic of Singapore's National Research Foundation through a grant to the Berkeley Education Alliance for Research in Singapore (BEARS) for the Singapore-Berkeley Building Efficiency and Sustainability in the Tropics (SinBerBEST) Program. BEARS has been established by the University of California, Berkeley as a centre for intellectual excellence in research and education in Singapore.

Disclosure statement

The authors have no financial interests to declare.

References

Armstrong, J.D., 1990. A new measure of uniformity for lighting installations. J. Illum. Eng. Soc. 19, 84–89. https://doi.org/10.1080/00994480.1990.10747967

Baxter, M.J., 1995. Standardization and transformation in principal component analysis, with applications to archaeometry. J. R. Stat. Soc. Ser. C Appl. Stat. 44, 513–527. https://doi.org/10.2307/2986142

BCA Green Mark, 2016. Green Mark: Non-residential buildings NRB: 2015. Technical guide and requirements. Building and Construction Authority, Singapore.
Bean, A.R., 1975. Utilance values and uniformity in a model room. Light. Res. Technol. 7, 169–178. https://doi.org/10.1177/096032717500700304
Bouveyron, C., Brunet-Saumard, C., 2014. Model-based clustering of high-dimensional data: A review. Comput. Stat. Data Anal. 71, 52–78. https://doi.org/10.1016/j.csda.2012.12.008
Bouveyron, C., Girard, S., Schmid, C., 2007. High-dimensional data clustering. Comput. Stat. Data Anal. 52, 502–519. https://doi.org/10.1016/j.csda.2007.02.009
Boyce, P., 2014. Editorial: Light distribution – a missing variable. Light. Res. Technol. 46, 617–617. https://doi.org/10.1177/1477153514556940
Canziani, R., Peron, F., Rossi, G., 2004. Daylight and energy performances of a new type of light pipe. Energy Build. 36, 1163–1176. https://doi.org/10.1016/j.enbuild.2004.05.001
CIBSE, 1994. The 1994 CIBSE interior lighting code. Health Estate J. J. Inst. Hosp. Eng. 50, 2–5.
Constantatos, B., 1982. Uniformity as the key element in present developments in lighting design: (or—Why there seems to be an apparent dichotomy between artificial and natural lighting schemes). Light. Res. Technol. 14, 102–105. https://doi.org/10.1177/096032718201400202
Daylight Metrics Committee, 2012. IES LM-83-12. Illuminating Engineering Society of North America, New York, United States.
Dewey, E.J., Littlefair, P.J., 1998. Rooflight spacing and uniformity. Light. Res. Technol. 30, 119–125. https://doi.org/10.1177/096032719803000305
Doulos, L., Tsangrassoulis, A., Topalis, F., 2008. Quantifying energy savings in daylight responsive systems: The role of dimming electronic ballasts. Energy Build. 40, 36–50. https://doi.org/10.1016/j.enbuild.2007.01.019
Ferguson, C.J., 2009. An effect size primer: A guide for clinicians and researchers. Prof. Psychol. Res. Pract. https://doi.org/10.1037/a0015808
Field, A., 2013. Discovering statistics using IBM SPSS statistics. SAGE Publications.
Freewan, A.A., 2010. Maximizing the lightshelf performance by interaction between lightshelf geometries and a curved ceiling. Energy Convers. Manag., Global Conference on Renewables and Energy Efficiency for Desert Regions (GCREEDER 2009) 51, 1600–1604. https://doi.org/10.1016/j.enconman.2009.09.037
Freewan, A.A., Shao, L., Riffat, S., 2008. Optimizing performance of the lightshelf by modifying ceiling geometry in highly luminous climates. Sol. Energy 82, 343–353. https://doi.org/10.1016/j.solener.2007.08.003
Hothorn, T., Everitt, B.S., 2009. A handbook of statistical analyses using R, Second Edition. ed. Taylor & Francis, Milton Park, United Kingdom.
Husson, F., Lê, S., Pagès, J., 2005. Confidence ellipse for the sensory profiles obtained by principal component analysis. Food Qual. Prefer. 16, 245–250. https://doi.org/10.1016/j.foodqual.2004.04.019
Jakubiec, J.A., Reinhart, C.F., 2011. DIVA 2.0: Integrating daylight and thermal simulations using Rhinoceros 3D, DAYSIM, and EnergyPlus, in: In: 12th Conference of International Building Performance Simulation Association. Presented at the Proceedings of Building Simulation 2011, Sydney, Australia, pp. 2202–2209.

Jolliffe, I.T., Cadima, J., 2016. Principal component analysis: a review and recent developments. Philos. Transact. A Math. Phys. Eng. Sci. 374. https://doi.org/10.1098/rsta.2015.0202

Kamaruzzaman, S.N., Edwards, R., Zawawi, E.M.A., Che-Ani, A.I., 2015. Achieving energy and cost savings through simple daylighting control in tropical historic buildings. Energy Build. 90, 85–93. https://doi.org/10.1016/j.enbuild.2014.12.045

Kurtay, C., Esen, O., 2017. A new method for light shelf design according to latitudes: CUN-OKAY light shelf curves. J. Build. Eng. 10, 140–148. https://doi.org/10.1016/j.jobe.2017.02.008

Lee, E.S., DiBartolomeo, D.L., Selkowitz, S.E., 1999. The effect of venetian blinds on daylight photoelectric control performance. J. Illum. Eng. Soc. 28, 3–23. https://doi.org/10.1080/00994480.1999.10748247

Lee, K., Kriegman, D.J., Ho, J., 2005. Acquiring linear subspaces for face recognition under variable lighting. IEEE Trans. Pattern Anal. Mach. Intell. 27, 684–698. https://doi.org/10.1109/TPAMI.2005.92

Lever, J., Krzywinski, M., Altman, N., 2017. Points of significance: Principal component analysis. Nat. Methods 14, 641–642. https://doi.org/10.1038/nmeth.4346

Liang, Y.C., Lee, H.P., Lim, S.P., Lin, W.Z., Lee, K.H., Wu, C.G., 2002. Proper orthogonal decomposition and its applications - Part I: Theory. J. Sound Vib. 252, 527–544. https://doi.org/10.1006/jsvi.2001.4041

Littlefair, P.J., Aizlewood, M.E., Birtles, A.B., 1994. The performance of innovative daylighting systems. Renew. Energy, Climate change Energy and the environment 5, 920–934. https://doi.org/10.1016/0960-1481(94)90113-9

Lynes, J.A., 1979. A sequence for daylighting design. Light. Res. Technol. 11, 102–106. https://doi.org/10.1177/14771535790110020101

Mahdavi, A., 1997. On the problem of operative information in CAAD, in: The 7th International Conference on Computer Aided Architectural Design Futures. Presented at the CAAD futures 1997, Springer, Munich Germany, pp. 231–244.

Mahdavi, A., Pal, V., 1999. Toward an Entropy-based light distribution uniformity indicator. J. Illum. Eng. Soc. 28, 24–29. https://doi.org/10.1080/00994480.1999.10748248

Mardaljevic, J., Heschong, L., Lee, E., 2009. Daylight metrics and energy savings. Light. Res. Technol. 41, 261–283. https://doi.org/10.1177/1477153509339703

Mathieu, J.-P., 1989. Statistical uniformity, a new method of evaluation. J. Illum. Eng. Soc. 18, 76–80. https://doi.org/10.1080/00994480.1989.10748762

McCormick, E., Jakubiec, J.A., Budig, M., 2017. Analysis of architectural façade elements in tropical climates for daylight, thermal comfort and passive climatization, in: Proceedings of 15th IBPSA Conference. Presented at the Building Simulation, International Building Performance Simulation Association, San Francisco, CA, USA, pp. 2540–2548. https://doi.org/10.26868/25222708.2017.730

Nabil, A., Mardaljevic, J., 2006. Useful daylight illuminances: A replacement for daylight factors. Energy Build., Special Issue on Daylighting Buildings 38, 905–913. https://doi.org/10.1016/j.enbuild.2006.03.013

Nabil, A., Mardaljevic, J., 2005. Useful daylight illuminance: a new paradigm for assessing daylight in buildings. Light. Res. Technol. 37, 41–57. https://doi.org/10.1191/1365782805li128oa

Nayar, S.K., Murase, H., 1994. Dimensionality of illumination manifolds in appearance matching, in: ORCV 1996. Presented at the International workshop on object representation in computer visio, Springer, Cambridge, UK, pp. 165–178.
Nicol, F., Wilson, M., Chiancarella, C., 2006. Using field measurements of desktop illuminance in European offices to investigate its dependence on outdoor conditions and its effect on occupant satisfaction, and the use of lights and blinds. Energy Build. 38, 802–813. https://doi.org/10.1016/j.enbuild.2006.03.014
Parpairi, K., Baker, N., Steemers, K., Compagnon, R., 2002. The Luminance Differences index: a new indicator of user preferences in daylit spaces. Light. Res. Technol. 34, 53–66. https://doi.org/10.1191/1365782802li030oa
Ramamoorthi, R., 2002. Analytic PCA construction for theoretical analysis of lighting variability in images of a Lambertian object. IEEE Trans. Pattern Anal. Mach. Intell. 24, 1322–1333. https://doi.org/10.1109/TPAMI.2002.1039204
Reinhart, C.F., Mardaljevic, J., Rogers, Z., 2006. Dynamic daylight performance metrics for sustainable building design. LEUKOS 3, 7–31. https://doi.org/10.1582/LEUKOS.2006.03.01.001
Rockcastle, S., Andersen, M., 2014. Measuring the dynamics of contrast & daylight variability in architecture: A proof-of-concept methodology. Build. Environ. 81, 320–333. https://doi.org/10.1016/j.buildenv.2014.06.012
Ryckaert, W.R., Lootens, C., Geldof, J., Hanselaer, P., 2010. Criteria for energy efficient lighting in buildings. Energy Build. 42, 341–347. https://doi.org/10.1016/j.enbuild.2009.09.012
Slater, A.I., Boyce, P.R., 1990. Illuminance uniformity on desks: Where is the limit? Light. Res. Technol. 22, 165–174. https://doi.org/10.1177/096032719002200401
SLL, 2012. The SLL code for lighting. Chartered Institution of Building Services Engineers (CIBSE).
Smith, L.I., 2002. Elementary linear algebra (Technical Report No. OUCS-2002-12), Computer Science Technical Report. Wiley, New York.
Sun, Y., Wu, Y., Wilson, R., 2017. Analysis of the daylight performance of a glazing system with Parallel Slat Transparent Insulation Material (PS-TIM). Energy Build. 139, 616–633. https://doi.org/10.1016/j.enbuild.2017.01.001
Tregenza, P., 2017. Uncertainty in daylight calculations. Light. Res. Technol. 49, 829–844. https://doi.org/10.1177/1477153516653786
Tregenza, P.R., 1999. Standard skies for maritime climates. Int. J. Light. Res. Technol. 31, 97–106. https://doi.org/10.1177/096032719903100304
Tregenza, P.R., 1986. Measured and calculated frequency distributions of daylight illuminance. Light. Res. Technol. 18, 71–74. https://doi.org/10.1177/096032718601800202
Tsang, E.K.W., Kocifaj, M., Li, D.H.W., Kundracik, F., Mohelníková, J., 2018. Straight light pipes' daylighting: A case study for different climatic zones. Sol. Energy 170, 56–63. https://doi.org/10.1016/j.solener.2018.05.042
Ullah, I., Lv, H., Whang, A.J.-W., Su, Y., 2017. Analysis of a novel design of uniformly illumination for Fresnel lens-based optical fiber daylighting system. Energy Build. 154, 19–29. https://doi.org/10.1016/j.enbuild.2017.08.066
USGBC, 2019. LEED BD+C: Healthcare | v4 - LEED v4 Daylight [WWW Document]. URL http://www.usgbc.org/credits/healthcare/v4-draft/eqc-0 (accessed 12.13.18).

Wang, Z., Bovik, A.C., Sheikh, H.R., Simoncelli, E.P., 2004. Image quality assessment: From error visibility to structural similarity. IEEE Trans. Image Process. 13, 600–612. https://doi.org/10.1109/TIP.2003.819861

Ward, G., Shakespeare, R., 1998. Rendering with Radiance: The art and science of lighting visualization. Morgan Kaufmann, Burlington, Massachusetts, United States.

Wentzell, P.D., Hou, S., 2012. Exploratory data analysis with noisy measurements. J. Chemom. 26, 264–281. https://doi.org/10.1002/cem.2428

Xue, P., Mak, C.M., Huang, Y., 2016. Quantification of luminous comfort with dynamic daylight metrics in residential buildings. Energy Build. 117, 99–108. https://doi.org/10.1016/j.enbuild.2016.02.026

Yao, Q., Zhong, B., Shi, Y., Ju, J., 2017. Evaluation of several different types of uniformity metrics and their correlation with subjective perceptions. LEUKOS 13, 33–45. https://doi.org/10.1080/15502724.2016.1172488

Yun, G.Y., Kong, H.J., Kim, H., Kim, J.T., 2012. A field survey of visual comfort and lighting energy consumption in open plan offices. Energy Build. 46, 146–151. https://doi.org/10.1016/j.enbuild.2011.10.035

Zhao, L., Yang, Y.-H., 1999. Theoretical analysis of illumination in PCA-based vision systems. Pattern Recognit. 32, 547–564. https://doi.org/10.1016/S0031-3203(98)00119-8

Zhu, L., Shao, Z., Sun, Y., Soebarto, V., Gao, F., Zillante, G., Zuo, J., 2018. Indoor daylight distribution in a room with integrated dynamic solar concentrating facade. Energy Build. 158, 1–13. https://doi.org/10.1016/j.enbuild.2017.10.008